Review DOI: 10.1557/jmr.2020.34

◆ FOCUS ISSUE

This section of Journal of Materials Research is reserved for papers that are reviews of literature in a given area.

HETEROGENEITY IN 2D MATERIALS

Heterogeneous deformation of two-dimensional materials for emerging functionalities

Jin Myung Kim^{1,a),c)}, Chullhee Cho^{2,c)}, Ezekiel Y. Hsieh², SungWoo Nam^{3,b)}

- ¹Department of Materials Science and Engineering, University of Illinois at Urbana-Champaign, Urbana, Illinois 61801, USA
- ²Department of Mechanical Science and Engineering, University of Illinois at Urbana-Champaign, Urbana, Illinois 61801, USA
- ³Department of Materials Science and Engineering, Department of Mechanical Science and Engineering, University of Illinois at Urbana-Champaign, Urbana, Illinois 61801, USA
- ^{a)}Address all correspondence to these authors. e-mail: jk25@illinois.edu
- ^{b)}e-mail: swnam@illinois.edu

Received: 19 December 2019; accepted: 14 January 2020

Atomically thin 2D materials exhibit strong intralayer covalent bonding and weak interlayer van der Waals interactions, offering unique high in-plane strength and out-of-plane flexibility. While atom-thick nature of 2D materials may cause uncontrolled intrinsic/extrinsic deformation in multiple length scales, it also provides new opportunities for exploring coupling between heterogeneous deformations and emerging functionalities in controllable and scalable ways for electronic, optical, and optoelectronic applications. In this review, we discuss (i) the mechanical characteristics of 2D materials, (ii) uncontrolled inherent deformation and extrinsic heterogeneity present in 2D materials, (iii) experimental strategies for controlled heterogeneous deformation of 2D materials, (iv) 3D structure-induced novel functionalities via crumple/wrinkle structure or kirigami structures, and (v) heterogeneous strain-induced emerging functionalities in exciton and phase engineering. Overall, heterogeneous deformation offers unique advantages for 2D materials research by enabling spatial tunability of 2D materials' interactions with photons, electrons, and molecules in a programmable and controlled manner.

Introduction: unique mechanical properties of 2D materials

Materials can exhibit drastically different characteristics depending on the dimensionality of their crystal structures [1]. Distinct from both bulk (3D) materials and low-dimensional materials prepared traditionally by simply reducing the size of 3D materials, two-dimensional (2D) materials exhibit unique mechanical, electrical, optical, and thermal characteristics because of quantum confinement effects and a lack of surface dangling bonds [2]. 2D materials are atomically thin, layered crystalline solids exhibiting intralayer covalent bonding and interlayer van der Waals interactions [3], offering high in-plane strength and out-of-plane flexibility. Thus, the unique characteristics of atomic thinness with high crystal and electronic quality in 2D materials show promise for exploring the coupling between mechanical deformations and emerging functionalities at the nanoscale such as electron transport, optical properties, and chemical phenomena.

Because of the atomically thin nature of 2D materials, external influences, especially mechanical deformation, can strongly impact their electronic properties. For example, strain-induced lattice distortions of graphene, a 2D sheet of covalently bonded carbon atoms in a hexagonal lattice, were found to create pseudo-magnetic fields and give rise to pseudo-quantum Hall effects [4, 5]. This demonstrated the importance of coupling between the mechanical and electronic properties in 2D materials and led to the development of "strain engineering," by which 2D materials are mechanically deformed to induce electronic structure changes. Further exploration of this field resulted in extensive exploration into the mechanical properties of various 2D materials.

The first definitive measurements of the mechanical properties of single-layer graphene were conducted using atomic force microscope (AFM) nanoindentation [6]. Graphene, which was first successfully isolated as a single atomic layer from its bulk materials via a micromechanical cleavage technique [7], has a predicted intrinsic strength exceeding that of

© Materials Research Society 2020 cambridge.org/JMR

c)These authors contributed equally to this work.



any other materials [8]. Static AFM deflection measurements of suspended graphene over microscale holes [Fig. 1(a)] enabled direct determination of elastic properties by minimizing the effects of sample geometry uncertainty and unknown load distributions, such as stress concentrations at clamping points. By pressing on the suspended sheet using AFM tips with calibrated spring constants, Young's modulus was extracted from the resultant force-displacement behaviors [6, 9]. Figure 1(b) shows the distribution of the extracted effective elastic modulus of graphene. Graphene exhibited Young's modulus of 1 TPa, establishing it as the strongest material ever measured [6]. Figure 1(c) shows Young's modulus and bending stiffness [2] of various 2D material monolayers other than graphene [10], including insulating/dielectric diatomic hexagonal boron nitride (h-BN) [11, 12], direct band gap transition metal dichalcogenide (TMD) monolayers, such as molybdenum disulfide (MoS₂) [13] and tungsten diselenide (WSe₂) [14], and monoatomic buckled crystals (Xenes) of phosphorene [15]. As shown in Figures. 1(c), 2(D) materials exhibit very low bending stiffness where they are at least seven orders-ofmagnitude lower than bulk materials including nanowire/ nanomembranes (e.g., InAs, GaAs, Ge, and Si nanowires or nanomembranes) and at least nineteen orders-of-magnitude lower than conventional III-V semiconductor compounds.

Inherent deformation of 2D materials

Prior to exploring mechanical deformation control via strain engineering of 2D materials, we must first consider the intrinsic/extrinsic uncontrolled deformations present in 2D materials. The stability of 2D layers had been a long-standing theoretical debate with planar graphene presumed to not exist in the free state due to thermodynamic instability under ambient conditions. Yet perfectly flat 2D crystals still cannot exist in the free state, according to both theory and experiments [16, 17, 18]. According to the Mermin–Wagner theorem [19], a 2D membrane can exist but will exhibit strong height fluctuations, resulting in

a tendency to be corrugated. It has been theoretically predicted [Fig. 2(A)] and experimentally observed [16] that 2D crystals become stable under small degree of corrugation, with out-of-plane deformations reaching 1 nm, leading to increased elastic energy but with suppressed thermal vibrations. However, it has been reported that such intrinsic instabilities (or ripples) of graphene can be fully suppressed by deposition onto an appropriate substrate [17]. Non-contact mode AFM results [Fig. 2(B)] showed that the height variation of graphene mechanically exfoliated on a mica substrate was less than 25 pm over micrometer-length scales, demonstrating "ultraflat" graphene. This result provides an insight into the importance of appropriate substrate selection, as atomically thin graphene may simply reflect the roughness of its underlying substrates.

Review

As the demand for scalable manufacturing of large-area and high-quality graphene increases, chemical vapor deposition (CVD) growth of graphene on catalytic substrates has been widely adopted because of its relatively large coverage, low cost, and efficiency [20]. However, uncontrolled extrinsic deformation, such as wrinkles, in CVD-grown 2D membranes can severely alter their performance, causing anisotropic electrical mobility, local charge accumulation, reduced mechanical strength, and diminished thermal conductivity [21]. Such wrinkles form because of the mismatch of thermal expansion coefficients (CTE) between CVD-grown graphene and its Cu growth substrate. During the cooling phase of the CVD process, this mismatch induces a strong compressive strain (~2% with a graphene growth temperature around 1000 °C) large enough to overcome the activation energy for wrinkle/buckle formation [Fig. 2(C)]. Wafer-scale growth of wrinkle-free single-crystal graphene on hydrogen-terminated germanium was reported, which was accomplished by using extremely weak adhesion, relatively small CTE mismatch, and unidirectional alignment enabled by the germanium(110) surface [22]. This revealed that wrinkle formation is also strongly dependent on the crystallographic orientation of the substrate. Similarly, wrinkle-free

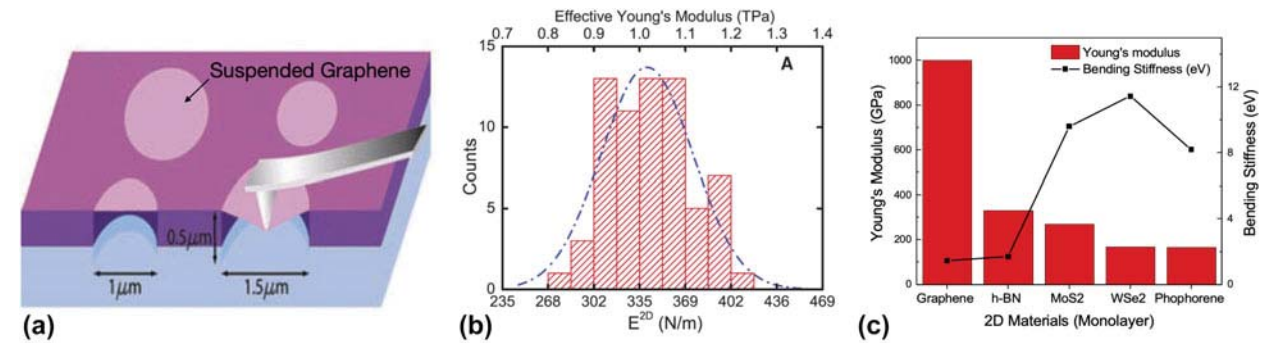


Figure 1: Mechanical properties of 2D materials. (a) Schematic illustration of AFM nanoindentation on suspended graphene over holes. (b) Histogram of elastic response of graphene. (c) Comparison of mechanical properties (Young's modulus and bending stiffness) of various 2D materials. (a, b) Reprinted with permission from Ref. 6.

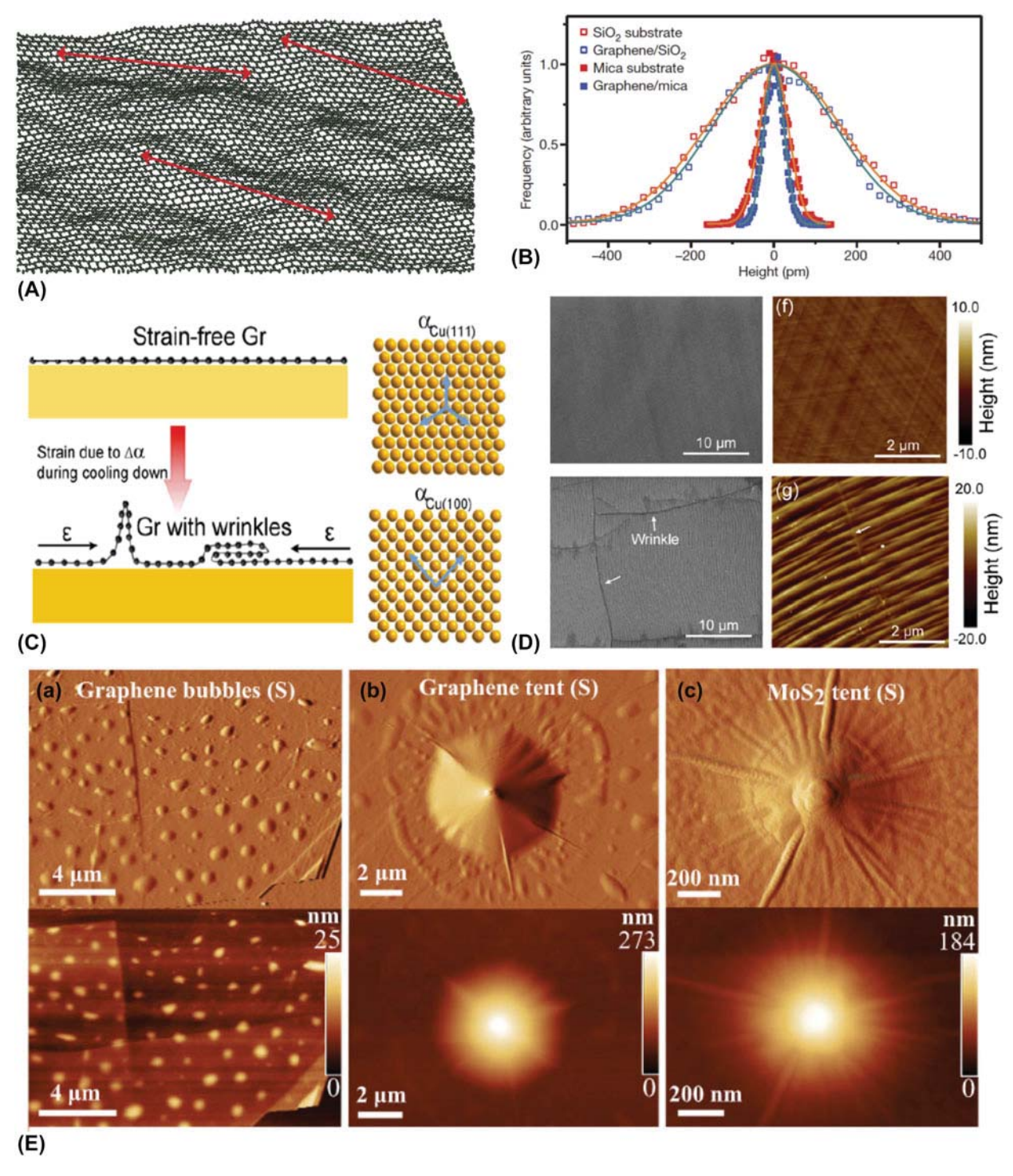


Figure 2: Intrinsic and extrinsic uncontrolled deformation of 2D materials. (A) Intrinsic ripples in monolayer graphene. (B) Substrate-dependent height variation of graphene and demonstration of ultraflat graphene deposited on a mica substrate. (C) Thermal expansion mismatch induced wrinkles during the CVD growth of 2D materials. (D) Crystallographic orientation-dependent wrinkle formation. (E) AFM topographic scans of transfer-induced nanoscale blisters, including bubbles and tents. (A) Reprinted with permission from Ref. 18. (B) Reprinted with permission from Ref. 17. (C, D) Reprinted with permission from Ref. 21. (E) Reprinted with permission from Ref. 26.

monocrystalline graphene was grown using Cu(111) thin film on a sapphire substrate [Fig. 2(D)]. Cu(111) [Fig. 2(D) bottom] exhibits relatively smaller thermal expansion than Cu(100)

[Fig. 2(D) top panel], and there is strong coupling between Cu(111) and graphene, enabling strain energy retention in the graphene lattice rather than wrinkle formation.

Another unexpected deformation present in 2D crystals emerges during the transfer from a growth substrate to a target substrate. 2D material-based approaches often require multiple transfers and precise manipulation of 2D materials in sample preparation. In this process, gas (air) or liquids (e.g., water and hydrocarbons) become inevitably trapped and spontaneously form nanometer-scale bubbles or tents [23, 24, 25, 26] as shown in Fig. 2(E). Gas-filled bubbles were generally deflated within a few hours, whereas liquid-filled bubbles showed less than 30% height change after three months [24]. These nanobubbles and nanotents have been used as a strain engineering tool to study 2D materials in response to nonuniform in-plane strain distributions, such as pseudo-magnetic fields [5], elastic properties [25], and large-scale quantum emitters [27]. However, although spontaneous nanobubbles/nanotents enabled observation of interesting effects on material characteristics, uncontrolled extrinsic deformation exhibits randomness to use outside of basic research of the strain effect. The difficulty in controlling the formation of nanoblisters (nanobubbles or nanotents) has remained a challenge. Thus, the existing lack of precise control over deformations and strain fields in 2D materials motivated exploration into approaches for controlling deformation in 2D materials.

Controlled deformation of 2D materials

While 2D materials' atomically thin nature inevitably causes uncontrolled intrinsic/extrinsic out-of-plane deformations in

multiple scales and varying morphologies, it also offers new opportunities for exploring heterogeneous deformations in programmable and scalable ways, which in turn allows for emerging physical phenomena or novel functionalities of deformed 2D materials. Prior to our discussion of specific spatial heterogeneity that modulates relevant properties, we will first review several important strategies for the controlled deformation of 2D materials in solid-state processes.

Epitaxial growth is one of the well-known approaches for creating strain in the vicinity of the interface of thin films with dissimilar lattice constants. Contrary to the vertical stacking, mostly observed in thin film epitaxy [28], weak van der Waals interaction between 2D material layers and easy interlayer sliding inhibit effective deformation of vertically stacked 2D heterostructures. However, epitaxial growth of lateral 2D heterostructures has been experimentally and theoretically demonstrated to impart different types of strains to adjacent 2D materials. Xie et al. investigated WS2-WSe2 lateral heterostructures grown by metal-organic chemical vapor deposition (MOCVD) [29]. Noticeably, the triangular 2D superlattice of WS2-WSe2 sustained a significant degree of lattice mismatch (~4%) in the absence of dislocation or other macroscopic defects. As a result, there was remarkable strain exerted on both WS₂ (tensile) and WSe₂ (compressive) which also caused highly periodic nanoripples on the WSe2 because of its very low bending stiffness and buckling instability [Fig. 3(a)].

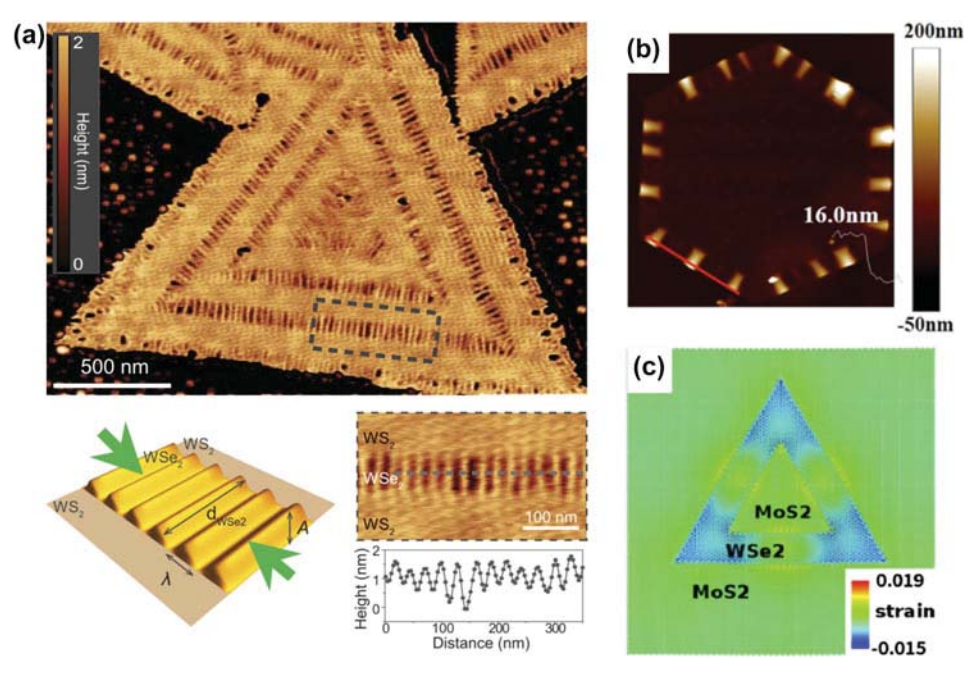


Figure 3: Epitaxial lateral 2D heterostructures with nanoscale ripples. (a) WS₂–WSe₂ lateral heterostructure showing rippling of WSe₂ due to lattice mismatch and compressive strain. AFM height map (top) and profile (right bottom) and schematic illustration of ripple formation (left bottom). (b) AFM height map for nanoplate Bi₂Se₃–Bi₂Te₃ lateral heterostructure with rippling along Bi₂Te₃ strips. (c) Molecular dynamics simulation of the strain distribution on a triangular 2D MoS₂–WSe₂ lateral heterostructure. (a) Reprinted with permission from Ref. 29. (b) Reprinted with permission from Ref. 30. (c) Reprinted with permission from Ref. 31.

4

Similarly, Bi₂Se₃/Bi₂Te₃ nanoplates laterally grown by the solution process (thickness ~16 nm) exhibited ripple structures because of a large lattice mismatch (~5.9%) [Fig. 3(b)] [30]. Interestingly, the ripple wavelength and amplitude were highly tunable by changing the Bi₂Te₃ strip width, with a structure highly predictable by continuum mechanics calculations. In a theoretical approach, molecular dynamics (MD) simulation also demonstrated misfit strain-induced buckling of 2D lateral heterostructures [31], which revealed exponential decay of tensile/compressive strain from the lateral interface with a strain decay length of 1.5 nm and a critical ripple generation width of 11.5 nm in the MoS2-WSe2 system. In addition to parallel configurations of 2D heterostructures, triangular lateral heterostructures were examined in the MD simulation, which showed out-of-plane buckle formation in the regions with larger lattice constants (i.e., compressive strain), similar to the reported experimental results [Fig. 3(c)]. On the other hand, Zhang et al. [100] reported that lateral p-n junctions of WSe2-MoS2 heterostructures (lattice mismatch ~3.8%) can only sustain 1.76% strain, while misfit dislocation partially released the remnant strain energy. The differing tendency of those lateral heterostructures, particularly in terms of the presence of energy-releasing defects, might be attributed to different growth processes, superlattice dimensions, or underlying substrates.

Another approach for creating controlled deformations of 2D materials is to use pre-patterned, 3D-microstructured substrates. There have been various types of nanostructured templates for tunable strain and properties, such as nanorods/nanotents [32, 33, 34, 35], nanogaps [36], nanowires [37], and nanocones [38]. Figure 4(A) shows graphene nanotents

suspended over high-aspect-ratio SiO₂ nanopillars [35]. It was revealed that the geometry of nanopillar arrays determined how graphene was deformed on the substrate, including conformal deformations, partial collapses, and suspended configurations. Similarly, Li et al. reported periodically strained MoS₂ monolayers on SiO₂ nanocone structures [Fig. 4(B)] [38]. Because of the capillary force-induced conforming of MoS₂ onto the nanopatterns, the resultant artificial lattice of MoS₂ successfully induced tensile strain in MoS2, which was verified using photoluminescence (PL)/Raman characterization and scanning tunneling microscope (STM) analysis. Recently, Liu et al. also demonstrated nanoscale roughness control of dielectric layers for MoS₂ field-effect transistors (FETs) [39]. The surface roughness from 0.1 to 2 nm was tuned by differing dielectric materials or pre-patterning fabrication, which enhanced the field-effect mobility of MoS2 FETs by an order of magnitude higher than conventional values because of the heterogeneous deformation and localized strain of MoS₂.

While the most of templating approaches use viscoelastic stamping or simple wet transfers, further improvement in interfacial integrity and reduced damage of suspended 2D materials on 3D structures are important for precisely controlled deformation, particularly in high-aspect-ratio structures. Choi et al. investigated graphene integrated with 3D microstructured surfaces via stepwise swelling, shrinking, and adaptation processes [Fig. 4(C)] [40]. Specifically, a pre-patterned 3D elastomer substrate was first swollen with solvent before graphene was transferred onto it. While the as-transferred graphene was first suspended over the complex 3D structure without making conformal contact, post shrinkage of the graphene/substrate caused by evaporation of the absorbed

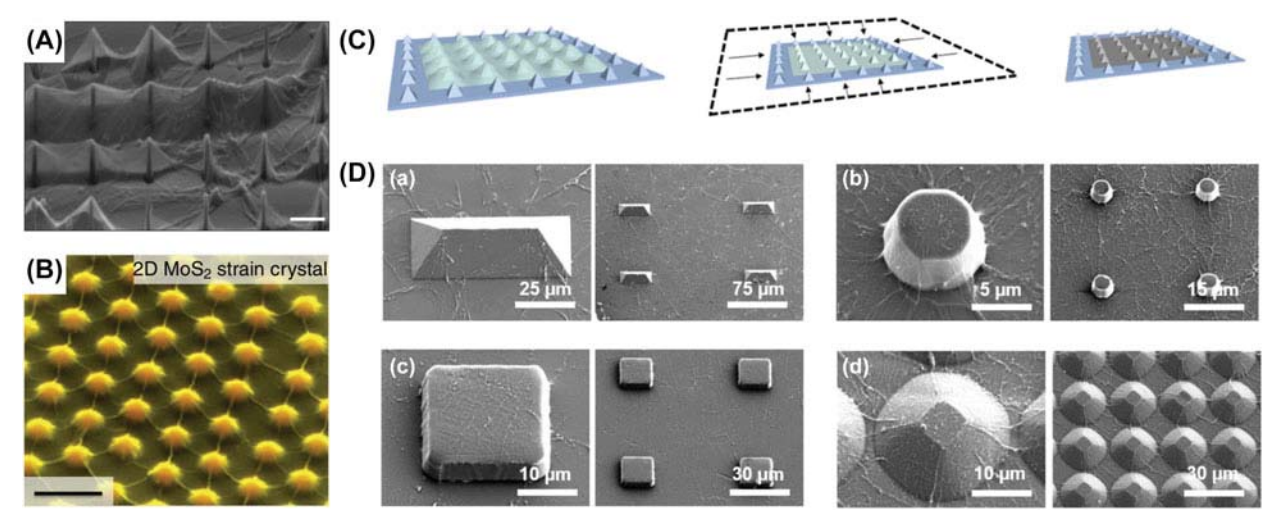


Figure 4: Heterogeneous deformation of 2D materials on 3D architecture. (A) Scanning electron microscope (SEM) image of a graphene nanotent on a SiO_2 nanopillar. (B) False color SEM image of monolayer MoS_2 transferred onto a SiO_2 nanocone structure. (C) Schematic diagram of high integrity 3D architecturing via swelling, shrinking, and adaptation. (D) SEM images of graphene on various 3D structures prepared by the sequential process shown in (C). (A) Reprinted with permission from Ref. 35. (B) Reprinted with permission from Ref. 38. (C, D) Reprinted with permission from Ref. 40.

solvent enabled the graphene to be gradually integrated onto the surface of the 3D structure (adaptation step). Figure 4(D) shows the successfully adapted graphene, even over the sharp and dense edges of the 3D structures, because of reduced capillary and tensile stress in the graphene during the drying step.

Buckle delamination and conformal deformation are additional important and versatile approaches for enabling heterogeneous deformation of 2D materials as tensile/compressive strains are applied alternatively to crests or valleys of wrinkle/ crumple structures. In general, shape-memory polymers or prestrained elastomers are used as the substrate to achieve wrinkle/crumple structures, with an optional stiff skin layer between the 2D materials and the substrate. Releasing the prestrain forms a crumple structure because of the modulus mismatch between the softer substrate and the stiff skin layer or 2D material. Figure 5(a) demonstrates that shrinkage of a prestrained shape-memory polymer can deform 2D materials in either uniaxial or biaxial direction [41, 42]. By heating above the glass transition temperature of prestrained polystyrene (PS), graphene/graphite lateral heterostructures were buckle delaminated because of macroscopic compressive strain (~70%), resulting in crumple structures [Fig. 5(b)]. This method not only maintains the electrical properties of the 2D materials but also allows for high tunability of the 3D architecture by changing the degree of shrinkage, thickness of 2D layers, and the local/global heating regime. Furthermore, another degree of freedom for tailoring the multiscale hierarchical 3D structure can be endowed by depositing a different thickness skin layer on top of the shape polymer [43, 44]. Figure 5(c) shows a spatially heterogeneous crumple structure of graphene on a fluorocarbon (CF_x)/PS substrate, which was enabled by stepwise patterning of differing fluorocarbon skin layer thicknesses.

In additional to shape-memory polymers, elastomeric substrates [e.g., polydimethylsiloxane (PDMS) and very high bond (VHB) films] can be used to generate crumple structures by prestretching the substrates, transferring the 2D materials, and then releasing the prestrain [45, 46, 47, 48, 49, 50, 51, 52, 53, 54, 55, 56]. A major benefit of elastomeric substrates is that they allow for dynamic tuning and reversible mechanical reconfiguring of heterogeneous deformation and strain in 2D materials, whereas the large Poisson effect can generate transverse cracks in the case of uniaxial wrinkle/crumple structures. In contrast to the efforts thus far to avoid cracks or macroscopic defects in the crumple structure, Leem et al. demonstrated the use of cracks for heterogeneous crumple formation of graphene. To accomplish this, they first formed a stiff silica skin layer on unstretched siloxane-based elastomers, followed by post-stretching and graphene transfer [Fig. 5(d)] [52]. The post-stretching caused cracks in the skin layer, allowing the compressive strains in the graphene to be highly localized over

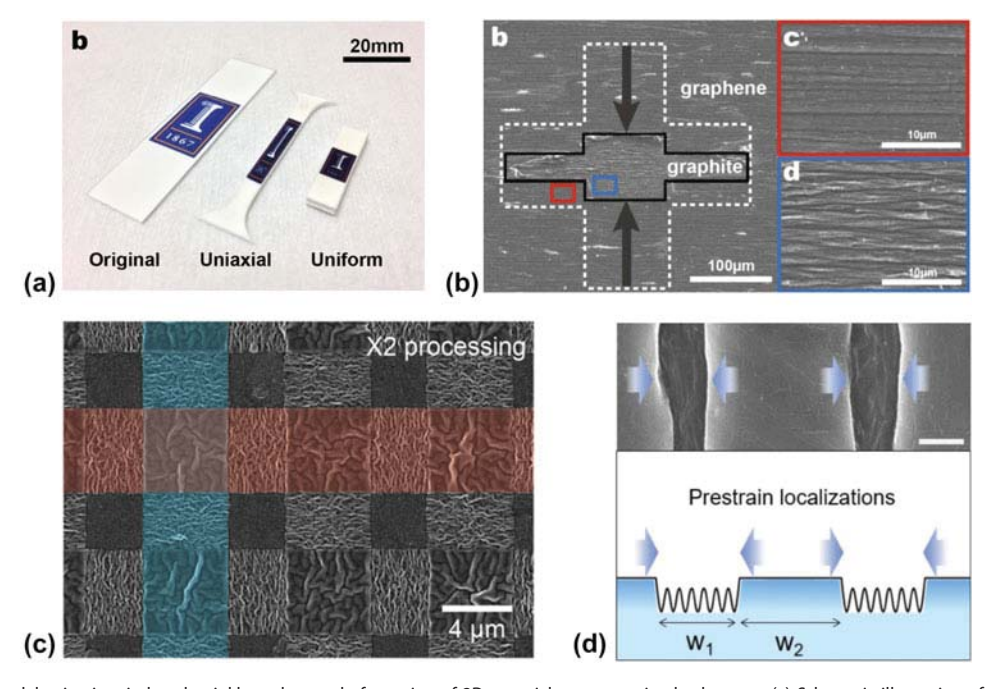


Figure 5: Buckle delamination–induced wrinkle and crumple formation of 2D materials on prestrained substrates. (a) Schematic illustration of the crumpling of graphene via shrinkage of a shape-memory polymer. (b) Concomitant crumpling of a graphene/graphite heterostructure with different crumple dimensions due to differing thicknesses. (c) Heterogenous graphene crumples formed by different thicknesses of a fluorocarbon skin layer on a shape-memory polymer. (d) Localized graphene wrinkles on an elastomeric substrate created by cracking a stiff SiO₂ skin layer. (a, b) Reprinted with permission from Ref. 41. (c) Reprinted with permission from Ref. 42. (d) Reprinted with permission from Ref. 52.



the crack regions, whereas the graphene on uncracked ${\rm SiO_2}$ regions maintained its flat structure.

We have discussed three important strategies for controlling deformation of 2D materials including epitaxial growth of lateral heterostructures, templating on 3D pre-patterned substrates, and shrinkage of prestrained substrates. In addition, there are other approaches to control deformation via liquid or colloidal processing such as crumpled microballs [57], liquidphase shrinkage of wrinkles [58], and transfer-induced wrinkles driven by substrate hydrophilicity [59], which have not been extensively discussed in this review. All the aforementioned deformation strategies enable control of the spatial heterogeneity of 2D materials in multiple length scales with programmed out-of-plane deformation. As a consequence, we can expect that the resultant macroscopic 3D structures or nanoscale in-plane strains may modulate 2D material interactions with external stimuli and working environments (e.g., light, electric bias, and liquid molecules) and induce new functionalities of 2D materials, which will be discussed in the following sections.

Structure-induced functionality of 2D materials

Structuring of 2D materials, including crumpling as discussed in the previous section, enables advanced optoelectronic and photonic applications owing to the structure-driven modifications of plasmonic resonance and material densifications. It has been demonstrated that mechanical crumpling of graphene can be used to create different surface structures while maintaining reversibility [41, 45, 49, 60], allowing for tunable plasmonic and optical properties. Recently, strong plasmonic resonances with broadband tunability were realized with the use of such mechanical reconfigurability of crumpled graphene [61]. Simulations showed that crumpled structures enable spectral tunability for plasmonic resonances from mid- to near-infrared ranges due to the shape-induced efficient coupling of light to the graphene plasmons and the subsequent strong confinement of the excited plasmons in crumpled graphene. As shown in the near-field distribution of graphene plasmons [Fig. 6(a)], crumpled graphene exhibited strong plasmon confinement with a high near-field intensity enhancement of $\sim 1 \times 10^4$ in the apex and valley regions of crumpled graphene structures. Furthermore, as the aspect ratios of the crumple height-towavelength increased from 0.25 to 2.0, the plasmonic resonance wavelength redshifted from 4.5 to 11.3 µm, suggesting a structurally dependent functionality/tunability of both far- and near-field plasmonic resonances.

Large stretchability and mechanical reconfigurability enabled by crumpled structures of 2D materials also allow for spectral emissivity tuning [50] owing to the mediated interference with incident light and surface structures. A recent study on emissivity control by mechanical reconfiguration of graphene enabled selective emitters that can affect the radiative cooling and heating management within solar irradiance and atmospheric transmissions. The capability of stretching and releasing induced dynamic topographic changes further enabled ultraviolet to mid-infrared emissivity control [Fig. 6(b)]. Periodic topography induced significant emissivity changes because of the modified interference with light and selective transmissivity reductions. The emissivity spectrum of crumpled graphene was tuned by controlling the pitch of the crumples, their predominant geometric parameter. As the pitch increased, the spectral region dominated by the diffraction-induced peaks shifted to longer wavelengths and narrowed the high emissivity region. The emissivity variations were a result of multiple diffraction and interference phenomena of photons over adjacent crumple features, demonstrating a novel functionality induced by structural changes of 2D materials.

Review

In addition to optical absorption tuning via structuring 2D materials, crumpled 2D materials in photodetectors showed mechanical tunability of optical absorption and further enhanced strain-tunable photoresponsivity [45, 49, 51]. Photoresponsivity was increased by more than 400% owing to increased graphene's surface areal density [45] with strain. This was the first demonstration of photoresponsivity tuning of a 2D materialbased photodetector via strain engineering [Fig. 6(c)]. However, the limited photoabsorption of graphene still remains a challenge. To improve the photoresponsivity, various hybrid systems have been introduced. A hybrid structure of crumpled graphene integrated with gold nanoparticles was shown to have a more than 1200% increase in plasmonically enhanced photoresponsivity over graphene-only photodetectors [49]. Most recently, a hybrid photodetector system consisting of photonic nanostructures (i.e., colloidal photonic crystals) on crumpled graphene demonstrated a dual function of the color change and electrical signal change in response to applied strain. Such a unique combination enabled both direct visual perception of strain via color responsivity as well as electrically quantifiable strain measurements that outperformed crumpled graphene strain sensors by more than 100 times [51].

Another well-known structure-induced functionality is tunable wettability. The wettability of surfaces can be strongly affected by their surface roughness. The degree of tunability is important for many industrial applications including coating, printing, and lubrication [62]. For this reason, crumpled 2D materials have been explored for water contact angle (WCA) modulation. The WCA measured on multilayer graphene on biaxially pre-strained VHB polymeric substrates varied from 105° (unfolded or flat) to 152° with applied strain [Fig. 7(a)] [53]. The degree of crumpling additionally affected the degree of wettability of graphene [Fig. 7(a)]. When the graphene was flat, the water droplet made

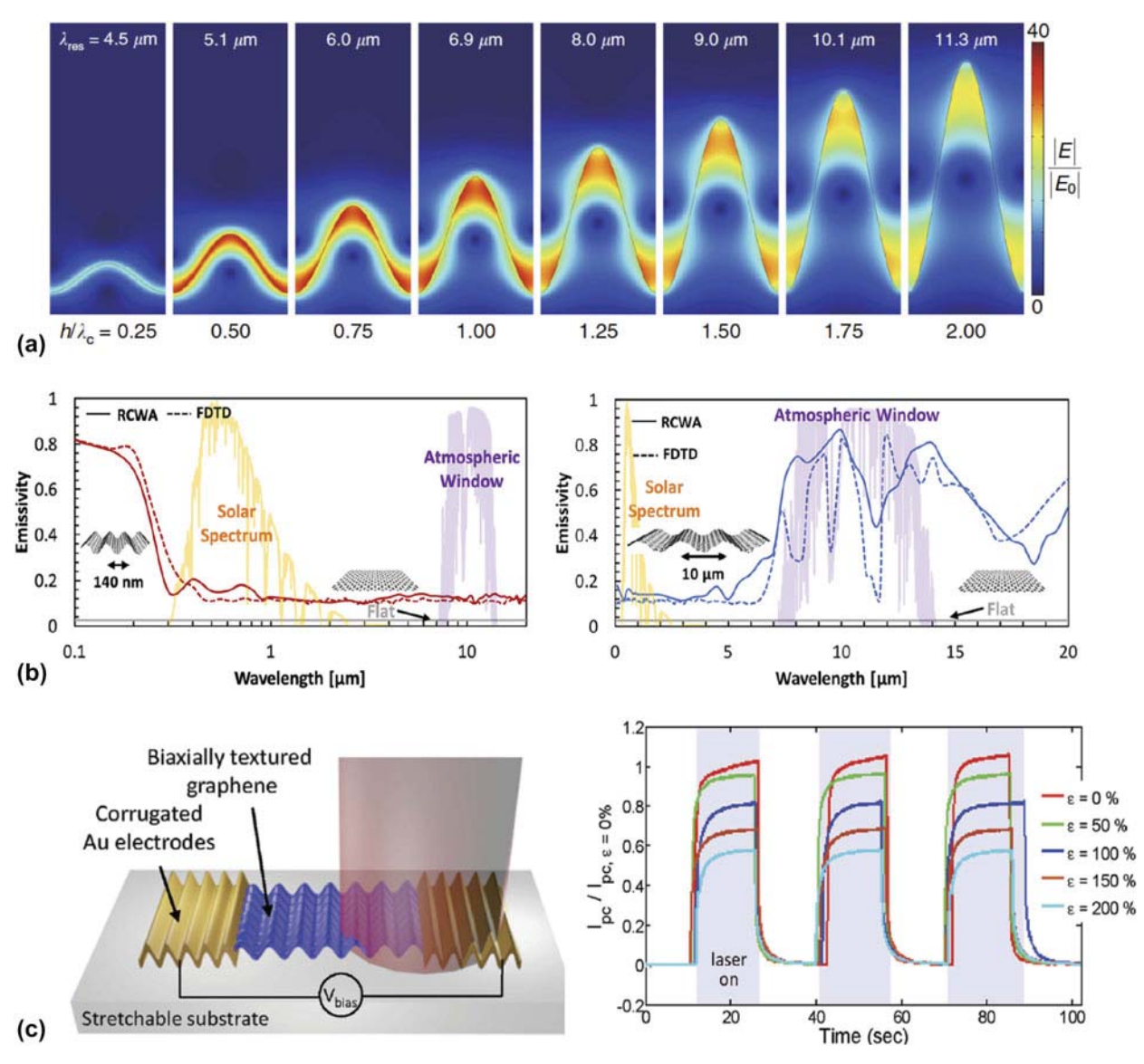


Figure 6: Structure-induced functionality of 2D materials: stretchable and strain-sensitive crumpled graphene. (a) Mechanically reconfigurable plasmonic resonances of uniaxially crumpled graphene structures showing variance with respect to height-to-wavelength (h/λ_c) ratio. λ_{res} is the plasmonic resonance wavelength. (b) Comparison of the computed emissivity values using rigorous coupled wave analysis (RCWA) and finite-difference time-domain (FDTD) methods under varying crumpling pitch. (c) Schematic illustrations of a strain-tunable photodetector based on crumpled graphene (left) and the resulting strain-tunable photoresponsivity (right). (a) Reprinted with permission from Ref. 61. (b) Reprinted with permission from Ref. 50. (c) Reprinted with permission from Ref. 45.

conformal contact to the graphene (Wenzel state), whereas when the graphene was highly crumpled, the water droplet remained in the Cassie–Baxter state, exhibiting superhydrophobicity (WCA > 150°). Furthermore, dual-scale control of morphology enhanced tunability compared with single-scale approaches [46]. The surface wettability could be dynamically and reversibly controlled by crumpling vertically-grown (i.e., nanoflower) MoS_2 , which exhibited a broadened WCA tunability range from 80 to 155° with strain dependency [Fig. 7(b)]. The crumpled nanoflower MoS_2 also demonstrated reduced contact angle hysteresis compared with as-prepared nanoflowers, demonstrating tunable interaction at the liquid–2D materials interface.

Last, apart from advances in stretchability and flexibility of 2D materials based nanodevices [2], there is an additional need to maintain desired device functionalities under various deformation. In other words, a novel functionality of strain insensitivity can be introduced by modulating strain distribution via structuring 2D material-based platforms. Recently, kirigami, an art of paper cutting to enable out-of-plane deformations of 2D thin films to create 3D structures, has been adopted as a strain-insensitive, reconfigurable means for various applications, including multidirectional photodetection/imaging [63] and motion detection [64]. The first demonstration of a kirigami structure using 2D materials was a highly stretchable graphene



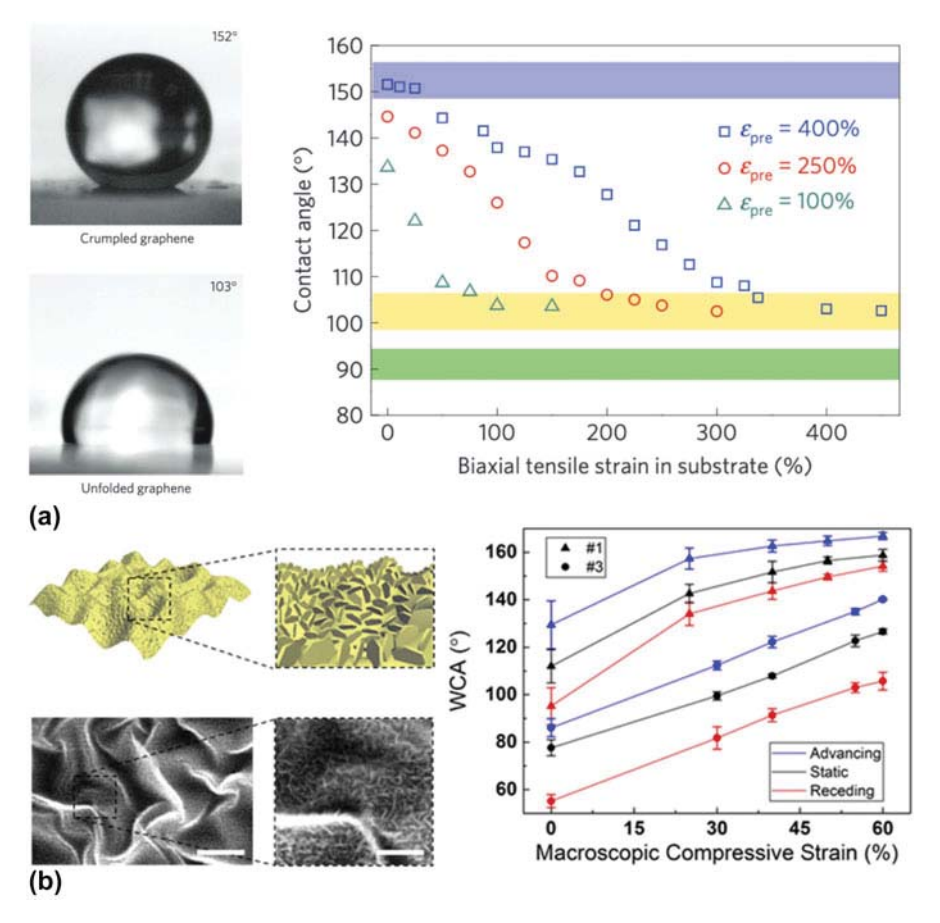


Figure 7: Structure-induced functionality of 2D materials: tunable wettability. (a) WCA of a water droplet on highly crumpled graphene (152°) and on unfolded graphene (103°). Contact angle measurement as a function of biaxial compressive strain in graphene (right). (b) Schematic illustration (top) and scanning electron microscope images (bottom) of crumpled nanoflower MoS₂. WCA measurement as a function of macroscopic compressive strain. (a) Reprinted with permission from Ref. 53. (b) Reprinted with permission from Ref. 46.

transistor [Fig. 8(a) left panel] [65]. Liquid-gated electrical response measurements [Fig. 8(a) right panel] showed no significant change when the device was stretched up to 240%. This result implied that the graphene lattice experienced minimal strain because of the kirigami-inspired structure. More recently, a free-standing kirigami-inspired graphene electrode encapsulated in thin polyimide layers demonstrated strain-insensitive electrical performance up to 240% stretching and mixed-mode strains, including shear and 720° torsion [Fig. 8(b)] [66]. Notably, a solution-gated graphene FET developed using the same kirigami structure exhibited strain, torsion, and shear insensitivity. This was primarily achieved through a desired structuring of graphene, redistributing stress concentrations via out-of-plane buckling at the kirigami notches.

Strain-induced functionalities of 2D materials

We have discussed the functionalities that emerge due to heterogeneous out-of-plane deformations of atomically thin materials, enabled by wrinkles, crumples, and kirigami structures. Although these approaches exploit the effective coupling between macroscopic deformations and their corresponding properties, another crucial way of modifying the functionalities of 2D materials is to engineer their in-plane lattice strain. This has gained significant interest because the high strengths and flexibilities of atomically thin materials enable improved sensitivity and greater robustness to external strain when compared with conventional bulk materials. The resulting strain-induced modulations of electron/phonon band structures combined with heterogeneous deformations provide unique opportunities for controlling a wide variety of 2D material properties, including enhanced photosensitivity [67], increased hydrogen evolution reactivity [68], higher field-effect mobility [39], tunable photoluminescence [69], dynamic phase transitions under ambient conditions [70], and anisotropic thermal management [71, 72]. In this part of our review, we will discuss in detail the strain-induced exciton dynamics and phase transitions in 2D TMD semiconductors, with more focus on heterogeneous deformation. One can find other review articles regarding more general aspects of strain engineering for 2D materials [73, 74].

10



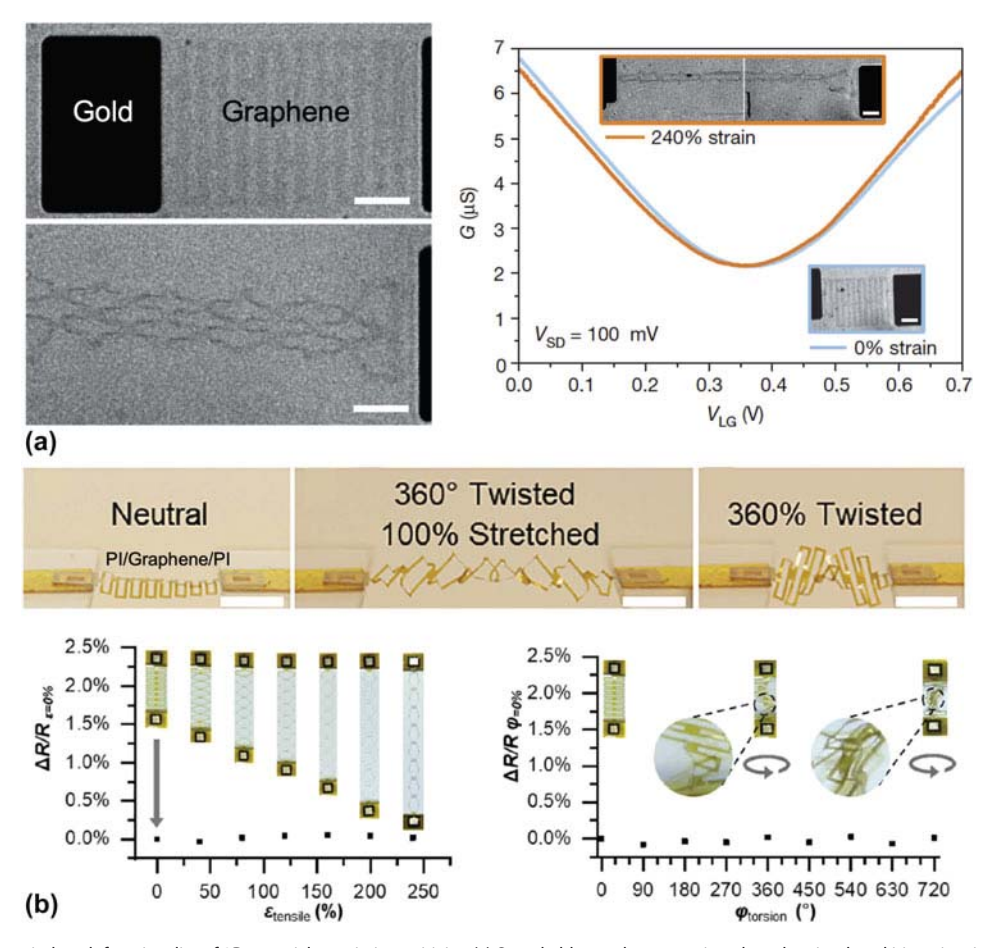


Figure 8: Structure-induced functionality of 2D materials: strain insensitivity. (a) Stretchable graphene transistor based on in-plane kirigami springs (left). Electrical response showing conductance (G) as a function of liquid-gate voltage (V_{LG}) with a source-drain bias (V_{SD}) of 100 mV. (b) Highly deformable free-standing kirigamiinspired graphene electrode (top). Strain-insensitive electrical performance (bottom) under stretching (left) and twisting (right) deformation. (a) Reprinted with permission from Ref. 65. (b) Reprinted with permission from Ref. 66.

Excitons, electron-hole pairs bound by Coulombic attraction, are highly important for understanding the optical and optoelectronic properties of 2D semiconductors because of their strong binding energy ($E_{\rm b} > 500$ meV) and enhanced stability even under ambient conditions, attributed to the reduced screening effects in lower dimensional structures [75]. In particular, the interactions of incident light and 2D semiconductors (e.g., absorption and photoluminescence) can be tuned by strain-induced modulations of the electron/ phonon band structures. For instance, uniaxial tensile strain to monolayer/bilayer MoS2 causes the splitting of the in-plane Raman peak (E') and linear decrease in exciton energy because of asymmetric lattice distortions and reduced optical band gap under tensile strain [69]. Interestingly, the PL intensity of MoS₂ dropped significantly under tensile strain, opposite to trend observed in WSe₂ [76], because the optically forbidden indirect $K\Gamma$ transition started to have a lower energy than the optically active direct KK transition. Another important aspect to be considered is exciton-phonon coupling [77]. The different PL characteristics of various 2D TMDs under strain (e.g., PL

linewidth, peak symmetry and radiative decay rates) were attributed to competition between momentum-forbidden intervalley transition and bright direct transition, as well as the effectiveness of intravalley phonon scattering (e.g., phonon band splitting). The reduced phonon scattering caused direct KK transition excitons to remain in the light cone and accelerated radiative decay.

While uniform deformation of 2D materials itself provides opportunities for controlling various PL characteristics, spatially heterogeneous deformation endows another important factor to strain-induced 2D exciton engineering, that is, strain gradient in the real space. This enables us to control exciton flux by prompting excitons to drift toward localized strain regions where they possess the lowest energy. Feng et al. theoretically proposed an exciton funneling-based 2D energy harvester [Fig. 9(a)] [78]. The indentation tip was used to generate heterogeneous strain around the tip, inducing a strain gradient up to 9% localized biaxial strain as shown in the color map on monolayer MoS2. The calculated absorption spectra [Fig. 9(b)] indicate continuous shifts to lower energy under

increasing tensile strain, enabling photon absorption with a wide range of wavelengths and, thus, effective solar energy harvesting. Furthermore, excitons excited at the wider band gap regions were subject to funneling toward the highly strained regions (i.e., narrower band gap), while the strong exciton binding energy prevented dissociation of excitons into individual electrons and holes until they reached the electronhole selective buffer layers at the tips [Fig. 9(c)].

The experimental evidence for exciton funneling has been suggested in various types of heterogeneous deformations such as buckle delamination and rigid templates. For instance, buckle delamination of few layered MoS₂ [55], WSe₂ [48], ReS₂ [56], and black phosphorus [47] on elastomeric substrates demonstrated that heterogeneous strain is exerted along the buckle structure, and the strain gradients between the crests and valleys of the buckles led to exciton drift toward lower energy regions. This was supported by Raman spectra [55, 79], AFM/PL profiles [48], and PL enhancement [56, 80]. Similarly, monolayer MoS2 on a SiO2 nanocone template revealed PL enhancement at the peaks of the nanocones with localized tensile strain [38]. Time-resolved spatial photoluminescence of WSe₂ on SiO₂ pillars revealed exciton drift toward the tensilestrained points, while strain also affected the diffusivity and mobility of excitons [81].

Exciton funneling in strained 2D materials has been widely investigated for single-photon emission at low temperature. In

single-photon emitters, photon distribution becomes antibunched and there is a reduced chance for simultaneous observation of more than one photon. Antibunched photons are of vital importance as the unit entity for quantum informatics and quantum cryptography. Thus, it drew unprecedented attention when 2D WSe2 layers exhibited characteristic quantum emitter properties at localized points at cryogenic temperatures [82, 83, 84, 85]. Following the initial observation, it was additionally found that nanoscale strain gradients play a significant role in quantum emitters because the energy gradients cause excitons to be localized and confined in nanoscale traps. There are several approaches for inducing highly localized strain for 2D quantum emitters, including nanorod arrays [32, 33, 34], nanogaps [36], nanowires [37], piezoelectric substrates [86], and microactuators with nanopyramids [87]. Figure 9(d) shows an AFM image of monolayer WSe₂ (dotted line) transferred over gold nanogaps (yellow bar) with a gap distance of 100 nm. The normalized PL intensity map measured at 10 K is presented in Fig. 9(e), which reveals stronger PL emission from WSe2 suspended over nanogaps than that of flat WSe2. The PL spectra are of very narrow linewidth and have highly polarized characteristics with respect to the nanogap direction. The nanogap-induced 2D quantum emitters also show photon counts less than unity at zero time delay as shown in the second-order correlation function $g^{(2)}(\tau)$ [Fig. 9(f)].

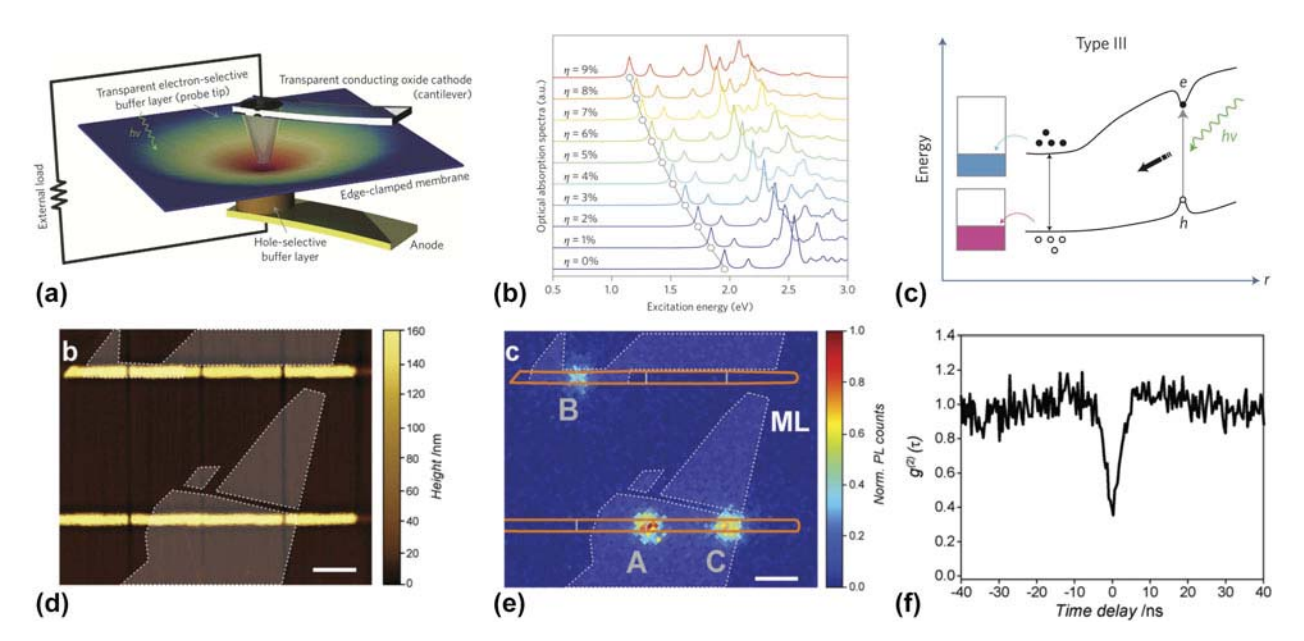


Figure 9: Heterogeneous strain engineering for exciton funneling and quantum emitters. (a) Schematic diagram of a funneling-based solar energy harvester using strained monolayer MoS₂. (b) Theoretically calculated absorption spectra of monolayer MoS₂ as a function of biaxial strain. (c) Schematic diagram of conduction/valence band edges of strained MoS₂ and the resulting exciton funneling along the energy gradient. Electron holes move in the same direction because of the strong exciton binding energy observed in 2D materials. (d) AFM height map of 2D WSe₂ suspended over a gold nanogap. (e) Normalized PL intensity map at cryogenic temperature, showing highly localized quantum emission at the nanogaps. (f) Second-order correlation function measured from 2D WSe₂ over a nanogap, revealing photon antibunching at zero time delay. (a–c) Reprinted with permission from Ref. 78. (d–f) Reprinted with permission from Ref. 36.

Another interesting feature of heterogeneously strained 2D materials is the dynamic modulation of phase stability. Particularly, the metal-to-insulator transition in 2D TMDs has been of great interest both for fundamental questions in how phase transition occurs by strain as well as for practical applications such as hydrogen evolution catalysis [88], Ohmic contact devices [89], and phase change transistors and memristors [90, 91]. The crystal structures of the semiconducting 2H and metallic 1T' phases in 2D TMDs are schematically illustrated in Fig. 10(a). The atomic stacking of metals and chalcogens in the 2H phase is $\alpha\beta\alpha\beta$, but it changes into an $\alpha\beta\gamma\alpha$ stacking sequence in the 1T and 1T' phase [70]. Most of those 2D TMDs have 2H phases that are stable polymorphs at room temperature and 1T' phases at high temperatures, but the energy barrier between the 2H and 1T' phases diminishes under strain, eventually resulting in a phase transition from the 2H to 1T' phase [70, 92]. Figure 10(b) illustrates the phase stability boundaries of various TMDs as a function of strain in a-axis or b-axis directions [directions shown in Fig. 10(a)]. In this theoretical diagram, only WTe2 has a stable 1T' phase at room temperature, whereas other 1T' TMDs only appear under specific applied strains in either direction. MoTe2 shows a smaller strain requirement for 2H-1T' phase transition, and the critical

strain for achieving 2H-1T' phase transition in MoTe₂ was estimated to range from 0.3% to 3% [70], making it as an appealing candidate for strain-induced phase change applications.

While the aforementioned theoretical simulations on strain-induced phase transition deal with uniform deformation or homogeneous strain, the experimental demonstration of strain-induced phase transition of 2D TMDs has been achieved mostly via heterogeneous, localized strain induced by sharp tips, propagating cracks, etc. For instance, Song et al. investigated phase transitions of 5- to 20-nm-thick MoTe₂ by applying localized strain with AFM tips and characterizing the in situ Raman spectra and electrical conductivities [93]. It was shown that only 0.2% of strain was required to promote phase transitions from the insulating 2H phase to the metallic 1T' phase [Figs. 10(c) and 10(d)], reducing the phase transition temperature from 855 °C to room temperature. Apte et al. also observed microscopic phase transitions in monolayer (Mo,W) Se₂ alloy (Mo:W = 2:1) at the strain-concentrated crack tips using scanning transmission electron microscopy (STEM) and molecular dynamics simulations [94]. They determined that the stress buildup around crack tips caused an irreversible phase transition from 2H to 1T phases in both MoSe₂ matrix and WSe2 patches [Fig. 10(e)]. More recently, a strain-induced

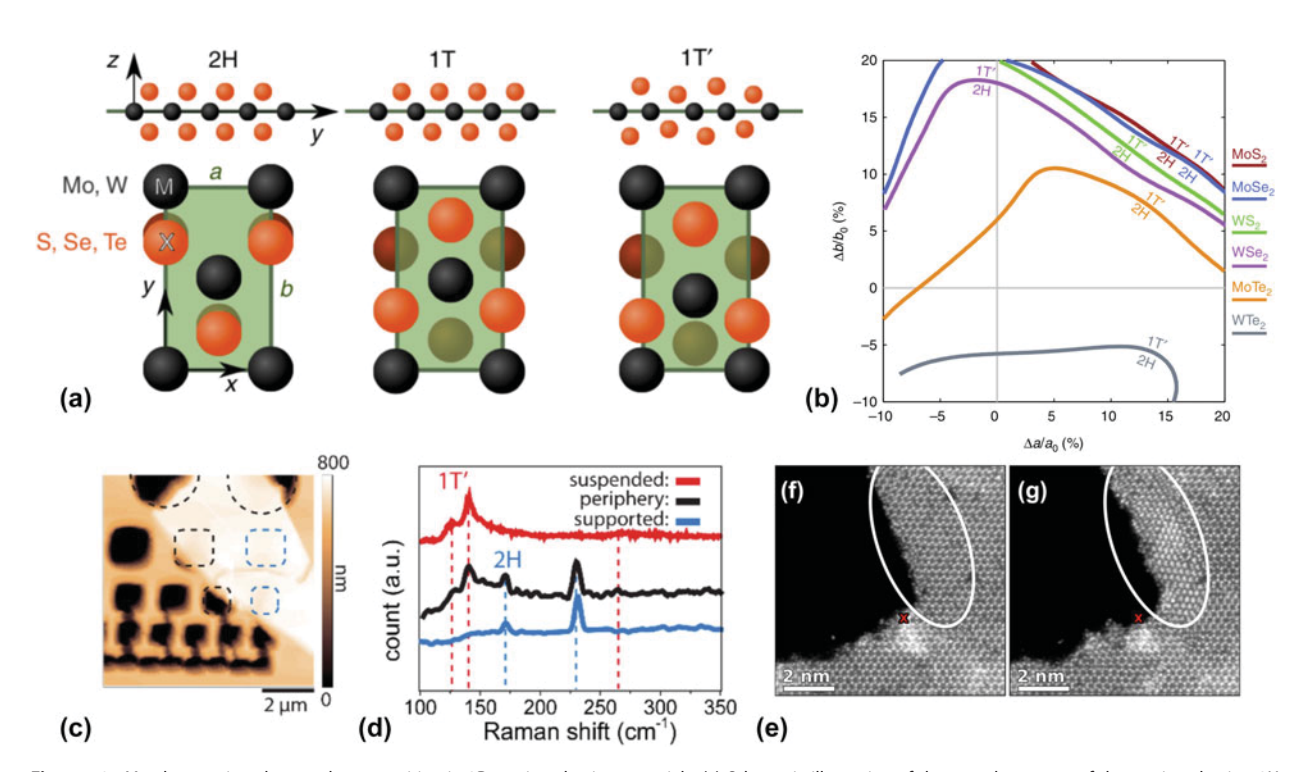


Figure 10: Metal-to-semiconductor phase transition in 2D semiconducting materials. (a) Schematic illustration of the crystal structure of the semiconducting 2H phase, metastable 1T phase, and stable, distorted metallic 1T' phase. (b) Theoretically simulated phase stability diagram with the locus of critical strain for phase transition in the *a*- and *b*-direction. (c) Thin MoTe₂ flake suspended over the Si patterned hole. (d) Raman spectra of MoTe₂ at different locations with inducing strain by AFM tip (~0.2% equiaxial strain). (e) Nanoscopic 2H–1T phase transition in (Mo,W)Se₂ near the propagating crack tip. (a, b) Reprinted with permission from Ref. 70. (c, d) Reprinted with permission from Ref. 93. (e) Reprinted with permission from Ref. 94.



phase change transistor was realized by electric field–induced strain on 13-nm-thick MoTe₂ [91]. Large in-plane tensile stress (0.58 GPa) was applied to MoTe₂ by the ferroelectric substrate and 35 nm of Ni contact pad, which generated 0.4% in-plane strain in MoTe₂ near the metal contact area. After several cycles, the device began to exhibit nonvolatile switching behavior because of the electrically conducting 1T' phase spreading from the metal contact area.

These experimental results may imply that localized high strain may facilitate the nucleation of phase transition, while the role of strain gradients in phase transition has yet to be investigated. In addition, it remains a challenge to realize spatially controlled phase transitions via precisely programmable local strain and strain gradients, which would allow for strain-induced memristors [90] and contact resistance–controlled devices [89, 95] as demonstrated in other 2D phase transition approaches.

Summary and perspectives

In conclusion, controlling the deformation of 2D materials with spatial heterogeneity is an effective and versatile approach for engineering functionalities via either macroscopic out-of-plane structures or lattice strains combined with strain gradients. Significant efforts have been devoted to understanding the unique mechanical characteristics of 2D materials and exploiting them to achieve programmable and precisely controlled deformation at multiple length scales. As we have discussed, heterogeneous deformation via epitaxial lateral growth, flexible substrates, and kirigami structures realized emerging properties such as confined plasmons, enhanced photoresponsivity, tunable wettability, and strain insensitivity. Furthermore, heterogeneous strain fields in 2D semiconductors offered varying opportunities for achieving exciton flux or localized exciton distribution, as well as dynamic phase transitions without requiring chemical or thermal treatments.

In addition to the efforts thus far, there are several perspectives for future research on heterogeneous deformation of 2D materials. First of all, extending the material palettes for controlled deformation beyond graphene and few TMDs is of great importance as it will yield more degrees of freedom for tuning diverse functionalities other than optical and electronic applications. For instance, there is a growing interest in 2D magnetism and ferromagnetic-antiferromagnetic transitions by means of strain engineering for improved controllability and higher Curie temperatures, which have been only demonstrated in theoretical simulations [96, 97]. Moreover, the anisotropic thermal conductivity in heterogeneously deformed 2D materials has been theoretically demonstrated to be very effective for nanoscale thermal management, but further experimental research must be performed for implementing strain architecture into thermal characterization [71, 72]. In addition to homogeneous 2D materials, artificially stacked or laterally grown 2D

heterostructures are also important candidates for heterogeneous deformation because of their combinatorial freedom and interesting physical phenomena such as long-lived interlayer excitons or angle-dependent Moiré potentials.

Review

Expanding the capabilities of controlled deformation in 2D materials will also require the development of deformation strategies compatible with varied operating conditions, such as at low/high temperatures, under extreme pressures, or submerged in fluids. For instance, many-body interactions or superfluidity of heterogeneously deformed 2D materials can be interesting subjects for condensed matter research because of the localized strain effects on various bosons and fermions, although they often require extreme cryogenic temperatures [98, 99]. Electrochemical properties such as supercapacitance or enhanced electric double layers (EDLs) of crumpled 2D materials in liquid phases are also intriguing research areas and will require a more rigorous understanding of how 2D material interactions with deforming substrates are influenced by the surrounding liquid structure and electrostatic forces.

Last, another important issue to investigate in the future is how to improve tunable deformations, such as with precise control of strain/structure, higher strains, and dynamic reconfigurability. As it has been recently demonstrated, 3D architecture combined with microelectromechanical systems (MEMSs) or piezoelectric devices can be a promising approach for enhanced precision via electrical control of strain and highly tunable functionalities (e.g., phase transition [91] and quantum emitters [87]). In addition, more conformal and high-aspect-ratio deformation that may induce higher strains and strain gradients than conventional approaches would offer even greater opportunities for strain engineering of excitons, phonons, and phase transitions to the extent only theoretical simulations have been demonstrated.

Acknowledgments

S.N. gratefully acknowledges support from the NSF (ECCS-1935775, CMMI-1554019, CMMI-1904216, DMR-1708852 and MRSEC DMR-1720633), AFOSR (FA2386-17-1-4071 and FA9550-18-1-0405), NASA ECF (NNX16AR56G), and ONR YIP (N00014-17-1-2830). C.C. gratefully acknowledge support from the NASA Space Technology Research Fellowship (80NSSC17K0149). This research was partially supported by the NSF through the University of Illinois at Urbana-Champaign Materials Research Science and Engineering Center DMR-1720633.

References

K.S. Novoselov, D. Jiang, F. Schedin, T.J. Booth,
 V.V. Khotkevich, S.V. Morozov, and A.K. Geim: Two-dimensional atomic crystals. *Proc. Natl. Acad. Sci. U. S. A.* 102, 10451 (2005).



- D. Akinwande, N. Petrone, and J. Hone: Two-dimensional flexible nanoelectronics. *Nat. Commun.* 5, 5678 (2014).
- Q.H. Wang, K. Kalantar-Zadeh, A. Kis, J.N. Coleman, and M.S. Strano: Electronics and optoelectronics of two-dimensional transition metal dichalcogenides. *Nat. Nanotechnol.* 7, 699 (2012).
- **4. F. Guinea, M.I. Katsnelson, and A.K. Geim**: Energy gaps and a zero-field quantum hall effect in graphene by strain engineering. *Nat. Phys.* **6**, 30 (2010).
- N. Levy, S.A. Burke, K.L. Meaker, M. Panlasigui, A. Zettl,
 F. Guinea, A.H. Castro Neto, and M.F. Crommie: Strain-induced pseudo-magnetic fields greater than 300 tesla in graphene nanobubbles. Science 329, 544 (2010).
- C. Lee, X. Wei, J.W. Kysar, and J. Hone: Measurement of the elastic properties and intrinsic strength of monolayer graphene. *Science* 321, 385 (2008).
- K.S. Novoselov, A.K. Geim, S. V Morozov, D. Jiang, Y. Zhang,
 S.V. Dubonos, I.V. Grigorieva, and A.A. Firsov: Electric field
 effect in atomically thin carbon films. *Science* 306, 666 (2004).
- 8. Q. Zhao, M.B. Nardelli, and J. Bernholc: Ultimate strength of carbon nanotubes: A theoretical study. *Phys. Rev. B: Condens. Matter Mater. Phys.* 65, 1 (2002).
- I.W. Frank, D.M. Tanenbaum, A.M. Van Der Zande, and P.L. McEuen: Mechanical properties of suspended graphene sheets. J. Vac. Sci. Technol., B: Microelectron. Nanometer Struct. 25, 2558 (2007).
- Y. Wei, B. Wang, J. Wu, R. Yang, and M.L. Dunn: Bending rigidity and Gaussian bending stiffness of single-layered graphene. *Nano Lett.* 13, 26 (2013).
- V. Vijayaraghavan and L. Zhang: Effective mechanical properties and thickness determination of boron nitride nanosheets using molecular dynamics simulation. *Nanomaterials* 8, 546 (2018).
- **12. L. Boldrin, F. Scarpa, R. Chowdhury, and S. Adhikari**: Effective mechanical properties of hexagonal boron nitride nanosheets. *Nanotechnology* **22**, 505702 (2011).
- **13. J.W. Jiang, Z. Qi, H.S. Park, and T. Rabczuk**: Elastic bending modulus of single-layer molybdenum disulfide (MoS₂): Finite thickness effect. *Nanotechnology* **24**, 435705 (2013).
- K. Lai, W.B. Zhang, F. Zhou, F. Zeng, and B.Y. Tang: Bending rigidity of transition metal dichalcogenide monolayers from firstprinciples. *J. Phys. D: Appl. Phys.* 49, 185301 (2016).
- D. Verma, B. Hourahine, T. Frauenheim, R.D. James, and T. Dumitrică: Directional-dependent thickness and bending rigidity of phosphorene. *Phys. Rev. B* 94, 121404(R) (2016).
- 16. J.C. Meyer, A.K. Geim, M.I. Katsnelson, K.S. Novoselov, T.J. Booth, and S. Roth: The structure of suspended graphene sheets. *Nature* 446, 60 (2007).
- 17. C.H. Lui, L. Liu, K.F. Mak, G.W. Flynn, and T.F. Heinz: Ultraflat graphene. *Nature* 462, 339 (2009).
- **18. A. Fasolino, J.H. Los, and M.I. Katsnelson**: Intrinsic ripples in graphene. *Nat. Mater.* **6**, 858 (2007).

 N.D. Mermin: Crystalline order in two dimensions. *Phys. Rev.* 176, 250 (1968).

- 20. W. Wang, S. Yang, and A. Wang: Observation of the unexpected morphology of graphene wrinkle on copper substrate. Sci. Rep. 7, 1 (2017).
- 21. B. Deng, Z. Pang, S. Chen, X. Li, C. Meng, J. Li, M. Liu, J. Wu, Y. Qi, W. Dang, H. Yang, Y. Zhang, J. Zhang, N. Kang, H. Xu, Q. Fu, X. Qiu, P. Gao, Y. Wei, Z. Liu, and H. Peng: Wrinkle-free single-crystal graphene wafer grown on strain-engineered substrates. ACS Nano 11, 12337 (2017).
- H. Germanium, J. Lee, E.K. Lee, W. Joo, Y. Jang, B. Kim, J.Y. Lim, S. Choi, S.J. Ahn, J.R. Ahn, M. Park, C. Yang, B.L. Choi, S. Hwang, and D. Whang: Wafer-scale growth of single-crystal. *Science* 344, 286 (2014).
- 23. H. Ghorbanfekr-Kalashami, K.S. Vasu, R.R. Nair, F.M. Peeters, and M. Neek-Amal: Dependence of the shape of graphene nanobubbles on trapped substance. *Nat. Commun.* 8, 15844 (2017).
- 24. D.A. Sanchez, Z. Dai, P. Wang, A. Cantu-Chavez, C.J. Brennan, R. Huang, and N. Lu: Mechanics of spontaneously formed nanoblisters trapped by transferred 2D crystals. *Proc. Natl. Acad. Sci. U. S. A.* 115, 7884 (2018).
- 25. E. Khestanova, F. Guinea, L. Fumagalli, A.K. Geim, and I.V. Grigorieva: Universal shape and pressure inside bubbles appearing in van der Waals heterostructures. *Nat. Commun.* 7, 12587 (2016).
- Z. Dai, Y. Hou, D.A. Sanchez, G. Wang, C.J. Brennan,
 Z. Zhang, L. Liu, and N. Lu: Interface-governed deformation of nanobubbles and nanotents formed by two-dimensional materials. *Phys. Rev. Lett.* 121, 266101 (2018).
- C. Palacios-Berraquero, D.M. Kara, A.R.P. Montblanch,
 M. Barbone, P. Latawiec, D. Yoon, A.K. Ott, M. Loncar,
 A.C. Ferrari, and M. Atatüre: Large-scale quantum-emitter arrays in atomically thin semiconductors. *Nat. Commun.* 8, 15093 (2017).
- 28. C.W. Bark, D.A. Felker, Y. Wang, Y. Zhangd, H.W. Jang, C.M. Folkman, J.W. Park, S.H. Baek, H. Zhou, D.D. Fong, X.Q. Pan, E.Y. Tsymbal, M.S. Rzchowski, and C.B. Eom: Tailoring a two-dimensional electron gas at the LaAlO₃/SrTiO₃ (001) interface by epitaxial strain. *Proc. Natl. Acad. Sci. U. S. A.* 108, 4720 (2011).
- 29. S. Xie, L. Tu, Y. Han, L. Huang, K. Kang, K.U. Lao, P. Poddar, C. Park, D.A. Muller, R.A. DiStasio, and J. Park: Coherent, atomically thin transition-metal dichalcogenide superlattices with engineered strain. *Science* 359, 1131 (2018).
- S. Lou, Y. Liu, F. Yang, S. Lin, R. Zhang, Y. Deng, M. Wang, K.B. Tom, F. Zhou, H. Ding, K.C. Bustillo, X. Wang, S. Yan, M. Scott, A. Minor, and J. Yao: Three-dimensional architecture enabled by strained two-dimensional material heterojunction. *Nano Lett.* 18, 1819 (2018).
- **31. J.W. Jiang**: Misfit strain-induced buckling for transition-metal dichalcogenide lateral heterostructures: A molecular dynamics study. *Acta Mech. Solida Sin.* **32**, 17 (2019).



- **32. S. Kumar, A. Kaczmarczyk, and B.D. Gerardot**: Strain-induced spatial and spectral isolation of quantum emitters in mono- and bilayer WSe₂. *Nano Lett.* **15**, 7567 (2015).
- 33. A. Branny, S. Kumar, R. Proux, and B.D. Gerardot: Deterministic strain-induced arrays of quantum emitters in a twodimensional semiconductor. *Nat. Commun.* 8, 15053 (2017).
- 34. Y. Luo, G.D. Shepard, J.V. Ardelean, D.A. Rhodes, B. Kim, K. Barmak, J.C. Hone, and S. Strauf: Deterministic coupling of site-controlled quantum emitters in monolayer WSe₂ to plasmonic nanocavities. *Nat. Nanotechnol.* 13, 1137 (2018).
- 35. A. Reserbat-Plantey, D. Kalita, Z. Han, L. Ferlazzo, S. Autier-Laurent, K. Komatsu, C. Li, R. Weil, A. Ralko, L. Marty, S. Guéron, N. Bendiab, H. Bouchiat, and V. Bouchiat: Strain superlattices and macroscale suspension of graphene induced by corrugated substrates. *Nano Lett.* 14, 5044 (2014).
- 36. J. Kern, I. Niehues, P. Tonndorf, R. Schmidt, D. Wigger, R. Schneider, T. Stiehm, S. Michaelis de Vasconcellos, D.E. Reiter, T. Kuhn, and R. Bratschitsch: Nanoscale positioning of single-photon emitters in atomically thin WSe₂. Adv. Mater. 28, 7101 (2016).
- 37. T. Cai, S. Dutta, S. Aghaeimeibodi, Z. Yang, S. Nah, J.T. Fourkas, and E. Waks: Coupling emission from single localized defects in two-dimensional semiconductor to surface plasmon polaritons. *Nano Lett.* 17, 6564 (2017).
- 38. H. Li, A.W. Contryman, X. Qian, S.M. Ardakani, Y. Gong, X. Wang, J.M. Weisse, C.H. Lee, J. Zhao, P.M. Ajayan, J. Li, H.C. Manoharan, and X. Zheng: Optoelectronic crystal of artificial atoms in strain-textured molybdenum disulphide. *Nat. Commun.* 6, 7381 (2015).
- T. Liu, S. Liu, K.H. Tu, H. Schmidt, L. Chu, D. Xiang,
 J. Martin, G. Eda, C.A. Ross, and S. Garaj: Crested twodimensional transistors. *Nat. Nanotechnol.* 14, 223 (2019).
- J. Choi, H.J. Kim, M.C. Wang, J. Leem, W.P. King, and
 Nam: Three-dimensional integration of graphene via swelling, shrinking, and adaptation. *Nano Lett.* 15, 4525 (2015).
- M.C. Wang, S. Chun, R.S. Han, A. Ashraf, P. Kang, and S. Nam: Heterogeneous, three-dimensional texturing of graphene. *Nano Lett.* 15, 1829 (2015).
- 42. J. Leem, M.C. Wang, P. Kang, and S. Nam: Mechanically self-assembled, three-dimensional graphene-gold hybrid nanostructures for advanced nanoplasmonic sensors. *Nano Lett.* 15, 7684 (2015).
- 43. S. Deng, D. Rhee, W-K. Lee, S. Che, B. Keisham, V. Berry, and T.W. Odom: Graphene wrinkles enable spatially defined chemistry. *Nano Lett.* 19, 5640 (2019).
- 44. W.K. Lee, J. Kang, K.S. Chen, C.J. Engel, W. Bin Jung, D. Rhee, M.C. Hersam, and T.W. Odom: Multiscale, hierarchical patterning of graphene by conformal wrinkling. *Nano Lett.* 16, 7121 (2016).
- **45. P. Kang, M.C. Wang, P.M. Knapp, and S.W. Nam:** Crumpled graphene photodetector with enhanced, strain-tunable, and

wavelength-selective photoresponsivity. *Adv. Mater.* **28**, 4639 (2016).

- 46. J. Choi, J. Mun, M.C. Wang, A. Ashraf, S-W. Kang, and S. Nam: Hierarchical, dual-scale structures of atomically thin MoS₂ for tunable wetting. *Nano Lett.* 17, 1756 (2017).
- 47. J. Quereda, P. San-Jose, V. Parente, L. Vaquero-Garzon, A.J. Molina-Mendoza, N. Agraït, G. Rubio-Bollinger, F. Guinea, R. Roldán, and A. Castellanos-Gomez: Strong modulation of optical properties in black phosphorus through strain-engineered rippling. Nano Lett. 16, 2931 (2016).
- 48. K.P. Dhakal, S. Roy, H. Jang, X. Chen, W.S. Yun, H. Kim, J. Lee, J. Kim, and J.H. Ahn: Local strain induced band gap modulation and photoluminescence enhancement of multilayer transition metal dichalcogenides. *Chem. Mater.* 29, 5124 (2017).
- M. Kim, P. Kang, J. Leem, and S.W. Nam: A stretchable crumpled graphene photodetector with plasmonically enhanced photoresponsivity. *Nanoscale* 9, 4058 (2017).
- 50. A. Krishna, J.M. Kim, J. Leem, M.C. Wang, S. Nam, and J. Lee: Ultraviolet to mid-infrared emissivity control by mechanically reconfigurable graphene. *Nano Lett.* 19, 5086 (2019).
- P. Snapp, P. Kang, J. Leem, and S.W. Nam: Colloidal photonic crystal strain sensor integrated with deformable graphene phototransducer. Adv. Funct. Mater. 28, 1902216 (2019).
- 52. J. Leem, Y. Lee, M.C. Wang, J.M. Kim, J. Mun, M.F. Haque, S-W. Kang, and S. Nam: Crack-assisted, localized deformation of van der Waals materials for enhanced strain confinement. 2D Mater. 6, 044001 (2019).
- 53. J. Zang, S. Ryu, N. Pugno, Q. Wang, Q. Tu, M.J. Buehler, and X. Zhao: Multifunctionality and control of the crumpling and unfolding of large-area graphene. *Nat. Mater.* 12, 321 (2013).
- 54. A.V. Thomas, B.C. Andow, S. Suresh, O. Eksik, J. Yin, A.H. Dyson, and N. Koratkar: Controlled crumpling of graphene oxide films for tunable optical transmittance. *Adv. Mater.* 27, 3256 (2015).
- 55. A. Castellanos-Gomez, R. Roldán, E. Cappelluti, M. Buscema, F. Guinea, H.S.J. Van Der Zant, and G.A. Steele: Local strain engineering in atomically thin MoS₂. Nano Lett. 13, 5361 (2013).
- 56. S. Yang, C. Wang, H. Sahin, H. Chen, Y. Li, S.S. Li, A. Suslu, F.M. Peeters, Q. Liu, J. Li, and S. Tongay: Tuning the optical, magnetic, and electrical properties of ReSe₂ by nanoscale strain engineering. *Nano Lett.* 15, 1660 (2015).
- R.L.D. Whitby: Chemical control of graphene architecture:
 Tailoring shape and properties. ACS Nano 8, 9733 (2014).
- 58. W. Chen, X. Gui, B. Liang, M. Liu, Z. Lin, Y. Zhu, and Z. Tang: Controllable fabrication of large-area wrinkled graphene on a solution surface. ACS Appl. Mater. Interfaces 8, 10977 (2016).
- 59. F. Guinea, B. Horovitz, and P. Le Doussal: Gauge fields, ripples and wrinkles in graphene layers. *Solid State Commun.* 149, 1140 (2009).



- M.C. Wang, J. Leem, P. Kang, J. Choi, P. Knapp, K. Yong, and S.W. Nam: Mechanical instability driven self-assembly and architecturing of 2D materials. 2D Mater. 4, 022002 (2017).
- P. Kang, K.H. Kim, H.G. Park, and S.W. Nam: Mechanically reconfigurable architectured graphene for tunable plasmonic resonances. *Light: Sci. Appl.* 7, 17 (2018).
- 62. K.J. Kubiak, M.C.T. Wilson, T.G. Mathia, and P. Carval: Wettability versus roughness of engineering surfaces. Wear 271, 523 (2011).
- 63. W. Lee, Y. Liu, Y. Lee, B.K. Sharma, S.M. Shinde, S.D. Kim, K. Nan, Z. Yan, M. Han, Y. Huang, Y. Zhang, J.H. Ahn, and J.A. Rogers: Two-dimensional materials in functional three-dimensional architectures with applications in photodetection and imaging. *Nat. Commun.* 9, 1417 (2018).
- 64. W. Zheng, W. Huang, F. Gao, H. Yang, M. Dai, G. Liu, B. Yang, J. Zhang, Y.Q. Fu, X. Chen, Y. Qiu, D. Jia, Y. Zhou, and P. Hu: Kirigami-inspired highly stretchable nanoscale devices using multidimensional deformation of monolayer MoS₂. Chem. Mater. 30, 6063 (2018).
- 65. M.K. Blees, A.W. Barnard, P.A. Rose, S.P. Roberts, K.L. McGill, P.Y. Huang, A.R. Ruyack, J.W. Kevek, B. Kobrin, D.A. Muller, and P.L. McEuen: Graphene kirigami. Nature 524, 204 (2015).
- 66. K. Yong, S. De, E.Y. Hsieh, J. Leem, N.R. Aluru, and S. Nam: Kirigami-inspired strain-insensitive sensors based on atomicallythin materials. *Mater. Today* (2019). In press - https://doi.org/ 10.1016/j.mattod.2019.08.013.
- 67. P. Gant, P. Huang, D. Pérez de Lara, D. Guo, R. Frisenda, and A. Castellanos-Gomez: A strain tunable single-layer MoS₂ photodetector. *Mater. Today* 27, 8 (2019).
- 68. H. Li, C. Tsai, A.L. Koh, L. Cai, A.W. Contryman, A.H. Fragapane, J. Zhao, H.S. Han, H.C. Manoharan, F. Abild-Pedersen, J.K. Nørskov, and X. Zheng: Activating and optimizing MoS₂ basal planes for hydrogen evolution through the formation of strained sulphur vacancies. *Nat. Mater.* 15, 48 (2015).
- 69. H.J. Conley, B. Wang, J.I. Ziegler, R.F. Haglund, S.T. Pantelides, and K.I. Bolotin: Bandgap engineering of strained monolayer and bilayer MoS₂. Nano Lett. 13, 3626 (2013).
- K.A.N. Duerloo, Y. Li, and E.J. Reed: Structural phase transitions in two-dimensional Mo- and W-dichalcogenide monolayers. *Nat. Commun.* 5, 4214 (2014).
- C. Wang, Y. Liu, L. Li, and H. Tan: Anisotropic thermal conductivity of graphene wrinkles. *Nanoscale* 6, 5703 (2014).
- 72. L. Cui, X. Du, G. Wei, and Y. Feng: Thermal conductivity of graphene wrinkles: A molecular dynamics simulation. *J. Phys. Chem. C* 120, 23807 (2016).
- S. Deng, A.V. Sumant, and V. Berry: Strain engineering in twodimensional nanomaterials beyond graphene. *Nano Today* 22, 14 (2018).
- 74. Z. Dai, L. Liu, and Z. Zhang: Strain engineering of 2D materials: Issues and opportunities at the interface. Adv. Mater. 31, 1 (2019).

75. T. Mueller and E. Malic: Exciton physics and device application of two-dimensional transition metal dichalcogenide semiconductors. npj 2D Mater. Appl. 2, 1 (2018).

- 76. S.B. Desai, G. Seol, J.S. Kang, H. Fang, C. Battaglia, R. Kapadia, J.W. Ager, J. Guo, and A. Javey: Strain-induced indirect to direct bandgap transition in multilayer WSe₂. Nano Lett. 14, 4592 (2014).
- 77. I. Niehues, R. Schmidt, M. Drüppel, P. Marauhn, D. Christiansen, M. Selig, G. Berghäuser, D. Wigger, R. Schneider, L. Braasch, R. Koch, A. Castellanos-Gomez, T. Kuhn, A. Knorr, E. Malic, M. Rohlfing, S. Michaelis De Vasconcellos, and R. Bratschitsch: Strain control of exciton-phonon coupling in atomically thin semiconductors. Nano Lett. 18, 1751 (2018).
- J. Feng, X. Qian, C.W. Huang, and J. Li: Strain-engineered artificial atom as a broad-spectrum solar energy funnel. *Nat. Photonics* 6, 866 (2012).
- V.S. Mangu, M. Zamiri, S.R.J. Brueck, and F. Cavallo: Strain engineering, efficient excitonic photoluminescence, and exciton funnelling in unmodified MoS₂ nanosheets. *Nanoscale* 9, 16602 (2017).
- 80. A.V. Tyurnina, D.A. Bandurin, E. Khestanova, V.G. Kravets, M. Koperski, F. Guinea, A.N. Grigorenko, A.K. Geim, and I.V. Grigorieva: Strained bubbles in van der Waals heterostructures as local emitters of photoluminescence with adjustable wavelength. ACS Photonics 6, 516 (2019).
- 81. D.F. Cordovilla Leon, Z. Li, S.W. Jang, C.H. Cheng, and P.B. Deotare: Exciton transport in strained monolayer WSe₂. Appl. Phys. Lett. 113, 252101 (2018).
- 82. C. Chakraborty, L. Kinnischtzke, K.M. Goodfellow, R. Beams, and A.N. Vamivakas: Voltage-controlled quantum light from an atomically thin semiconductor. *Nat. Nanotechnol.* 10, 507 (2015).
- 83. Y.M. He, G. Clark, J.R. Schaibley, Y. He, M.C. Chen, Y.J. Wei, X. Ding, Q. Zhang, W. Yao, X. Xu, C.Y. Lu, and J.W. Pan: Single quantum emitters in monolayer semiconductors. *Nat. Nanotechnol.* **10**, 497 (2015).
- 84. M. Koperski, K. Nogajewski, A. Arora, V. Cherkez, P. Mallet, J.Y. Veuillen, J. Marcus, P. Kossacki, and M. Potemski: Single photon emitters in exfoliated WSe₂ structures. *Nat. Nanotechnol.* 10, 503 (2015).
- A. Srivastava, M. Sidler, A.V. Allain, D.S. Lembke, A. Kis, and
 A. Imamoglu: Optically active quantum dots in monolayer
 WSe₂. Nat. Nanotechnol. 10, 491 (2015).
- 86. O. Iff, D. Tedeschi, J. Martín-Sánchez, M. Moczała-Dusanowska, S. Tongay, K. Yumigeta, J. Taboada-Gutiérrez, M. Savaresi, A. Rastelli, P. Alonso-González, S. Höfling, R. Trotta, and C. Schneider: Strain-tunable single photon sources in WSe₂ monolayers. Nano Lett. 19, 6931 (2019).
- 87. H. Kim, J.S. Moon, G. Noh, J. Lee, and J-H. Kim: Position and frequency control of strain-induced quantum emitters in WSe₂ monolayers. *Nano Lett.* 19, 7534 (2019).



- 88. D. Voiry, H. Yamaguchi, J. Li, R. Silva, D.C.B. Alves, T. Fujita, M. Chen, T. Asefa, V.B. Shenoy, G. Eda, and M. Chhowalla: Enhanced catalytic activity in strained chemically exfoliated WS₂ nanosheets for hydrogen evolution. *Nat. Mater.* 12, 850 (2013).
- 89. S. Cho, S. Kim, J.H. Kim, J. Zhao, J. Seok, D.H. Keum, J. Baik, D.H. Choe, K.J. Chang, K. Suenaga, S.W. Kim, Y.H. Lee, and H. Yang: Phase patterning for ohmic homojunction contact in MoTe₂. Science 349, 625 (2015).
- 90. F. Zhang, H. Zhang, S. Krylyuk, C.A. Milligan, Y. Zhu, D.Y. Zemlyanov, L.A. Bendersky, B.P. Burton, A.V. Davydov, and J. Appenzeller: Electric-field induced structural transition in vertical MoTe₂- and Mo_{1-x}W_xTe₂-based resistive memories. *Nat. Mater.* 18, 55 (2019).
- 91. W. Hou, A. Azizimanesh, A. Sewaket, T. Peña, C. Watson, M. Liu, H. Askari, and S.M. Wu: Strain-based roomtemperature non-volatile MoTe₂ ferroelectric phase change transistor. *Nat. Nanotechnol.* 14, 668 (2019).
- 92. H.H. Huang, X. Fan, D.J. Singh, H. Chen, Q. Jiang, and W.T. Zheng: Controlling phase transition for single-layer MTe₂ (M = Mo and W): Modulation of the potential barrier under strain. *Phys. Chem. Chem. Phys.* 18, 4086 (2016).
- 93. S. Song, D.H. Keum, S. Cho, D. Perello, Y. Kim, and Y.H. Lee: Room temperature semiconductor-metal transition of MoTe₂ thin films engineered by strain. *Nano Lett.* 16, 188 (2016).

- 94. A. Apte, V. Kochat, P. Rajak, A. Krishnamoorthy, P. Manimunda, J.A. Hachtel, J.C. Idrobo, S.A. Syed Amanulla, P. Vashishta, A. Nakano, R.K. Kalia, C.S. Tiwary, and P.M. Ajayan: Structural phase transformation in strained monolayer MoWSe₂ alloy. ACS Nano 12, 3468 (2018).
- 95. H. Yang, S.W. Kim, M. Chhowalla, and Y.H. Lee: Structural and quantum-state phase transition in van der Waals layered materials. *Nat. Phys.* 13, 931 (2017).
- **96.** L. Webster and J.A. Yan: Strain-tunable magnetic anisotropy in monolayer CrCl₃, CrBr₃, and CrI₃. *Phys. Rev. B* **98**, 144411 (2018).
- Z. Wu, J. Yu, and S. Yuan: Strain-tunable magnetic and electronic properties of monolayer CrI₃. *Phys. Chem. Chem. Phys.* 21, 7750 (2019).
- L.V. Butov, C.W. Lai, A.L. Ivanov, A.C. Gossard, and
 D.S. Chemla: Towards Bose–Einstein condensation of excitons in potential traps. *Nature* 417, 47 (2002).
- 99. A.A. High, J.R. Leonard, A.T. Hammack, M.M. Fogler, L.V. Butov, A.V. Kavokin, K.L. Campman, and A.C. Gossard: Spontaneous coherence in a cold exciton gas. *Nature* 483, 584 (2012)
- 100. C. Zhang, M.Y. Li, J. Tersoff, Y. Han, Y. Su, L.J. Li, D.A. Muller, and C.K. Shih: Strain distributions and their influence on electronic structures of WSe2-MoS2 laterally strained heterojunctions. *Nat. Nanotechnol* 13, 152 (2018).